

Bottleneck crossover between classical and quantum superfluid turbulence

Victor S. L'vov,¹ Sergei V. Nazarenko,² and Oleksii Rudenko¹

¹*Department of Chemical Physics, The Weizmann Institute of Science, Rehovot 76100, Israel*

²*Mathematics Institute, University of Warwick, Coventry CV4 7AL, United Kingdom*

(Received 30 March 2007; revised manuscript received 25 June 2007; published 26 July 2007)

We consider superfluid turbulence near absolute zero of temperature generated by classical means, e.g., towed grid or rotation but not by counterflow. We argue that such turbulence consists of a *polarized* tangle of mutually interacting vortex filaments with quantized vorticity. For this system, we predict and describe a bottleneck accumulation of the energy spectrum at the classical-quantum crossover scale ℓ . Demanding the same energy flux through scales, the value of the energy at the crossover scale should exceed the Kolmogorov-41 (K41) spectrum by a large factor $\ln^{10/3}(\ell/a_0)$ (ℓ is the mean intervortex distance and a_0 is the vortex core radius) for the classical and quantum spectra to be matched in value. One of the important consequences of the bottleneck is that it causes the mean vortex line density to be considerably higher than that based on K41 alone, and this should be taken into account in (re)interpretation of new (and old) experiments as well as in further theoretical studies.

DOI: [10.1103/PhysRevB.76.024520](https://doi.org/10.1103/PhysRevB.76.024520)

PACS number(s): 67.40.Vs, 03.75.Lm

INTRODUCTION

Turbulence in superfluid liquids, such as ^4He and ^3He at very low temperatures, is an intriguing physical problem by itself because it comprises a system where the classical physics gets gradually transformed into the quantum one during the energy cascade from large to small scales.^{1,2} Recently, renewed broad interest on this subject has been motivated by an impressive progress in experimental techniques and new results, which has led in (at least) a conceptual understanding of classical and quantum limits of the superfluid turbulence, see, e.g., Refs. 3–15. Our paper, in turn, attempts to shed light on the physics of the superfluid turbulence behavior in the intermediate region near the classical-quantum crossover scale. We will see that transition of the turbulent energy cascade from the classical to the quantum scale is accompanied by a transition from strong hydrodynamic to weak wave turbulence with a bottleneck stagnation at the crossover scale.

Generally, the superfluid turbulence near zero temperature (for an introduction, see Refs. 1–3) can be viewed as a tangle of quantized vortex lines. If turbulence is produced by classical means and not by a counterflow, then at the scales much greater than the mean intervortex distance ℓ , the vortex discreteness is unimportant, so that the superfluid turbulence has essentially a classical character described by the Kolmogorov-41 (K41) approach.³ As we will see below, vortex lines in K41 state are polarized, i.e., tend to be codirected and organized in bundles. Since there is no viscosity or friction in a superfluid liquid near zero temperature, the classical energy cascade proceeds down the spectrum to the scale of order ℓ without dissipation, where the vortex discreteness and quantization effects become important. Even though some negligible part of the energy is lost, for example, by radiation of phonons generated due to slow vortex motions and intermittent vortex reconnections, the dominant part of the energy proceeds to cascade below the scale ℓ by means of nonlinearly interacting Kelvin waves,^{3,12,13,16} which were theoretically predicted in the 19th century¹⁷ and first experimentally observed by Hall.¹⁸ We emphasize that the fact that

the turbulence is produced by classical means is important here, because the resulting polarization inhibits further vortex reconnections and prevents rapid fragmentation into vortex loops with sizes smaller than ℓ . Thus, the main cascade carrier below scale ℓ will be Kelvin waves, which are generated by both slow vortex filament motions and fast (but rarer and localized) vortex reconnection events. Such reconnections produce sharp bends on the vortex lines and, therefore, generate a broader range of wavelengths than the slow vortex motions. However, the spectrum of the reconnection forcing decays with the wave number k sufficiently fast, and could effectively be thought as a large-scale source of Kelvin waves located at the crossover.¹⁵ Traditionally, the K41 spectrum is assumed to maintain its shape all the way down to the crossover scale, which, due to such an assumption, is calculated based on the K41 spectrum.³

In this paper, we demonstrate that, in contrast to the traditional viewpoint, the classical turbulent spectrum cannot be matched to its quantum counterpart at the same value of the energy flux because this flux requires much stronger levels of turbulence to be able to propagate through scales in sparse distributions of quantized vorticity. This leads to a bottleneck accumulation of the energy spectrum near the crossover scale which, in turn, significantly changes the position of the crossover ℓ (see Fig. 1) and the relationship between the energy flux and vorticity, which have widely been used in the interpretation of experimental results. Notice that the phenomenon of bottleneck accumulation between two energy-flux spectra of different nature is not peculiar to the superfluid turbulence and may occur, for example, in the atmosphere, ocean, and magnetosphere.

I. POLARIZATION OF THE VORTEX TANGLE

It is important to emphasize that the turbulence we consider in this paper is generated by classical means, e.g., by a towed grid¹¹ or by rotation,^{5–7} but not by a counterflow. In the latter case, the vortex tangle would be unpolarized and neither would we expect K41 spectrum for the scales greater

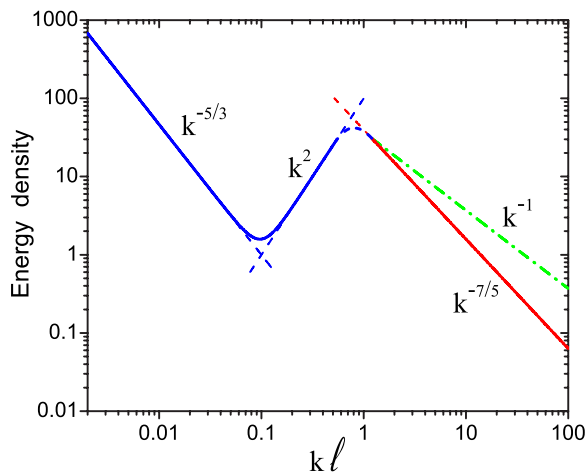


FIG. 1. (Color online) The energy spectra \mathcal{E}_k in the classical, $k < 1/\ell$, and quantum, $k > 1/\ell$, ranges of scales. Two straight blue (dark gray) lines in the classical range indicate the pure K41 scaling $\mathcal{E}_k^{K41} \propto k^{-5/3}$ [Eq. (12)] and the pure thermodynamic scaling $\mathcal{E}_k \propto k^2$. For the quantum range, the red (gray) solid line indicates the Kelvin wave cascade spectrum [Eq. (11)] (slope $-7/5$), whereas the green (light gray) dash-dotted line marks the spectrum corresponding to the noncascading part of the vortex tangle energy (slope -1).

than ℓ (K41 is polarized, see below) nor would we expect Kelvin waves to be important for the scales below ℓ (reconnections would be more important, see Ref. 19). On the other hand, polarization of the vortex tangle allows to shape large-scale vortex motions characteristic to the K41 cascade, and it also inhibits local reconnections and makes Kelvin waves a dominant vehicle for the turbulent energy cascade toward the small scales. Thus, let us consider the phenomenon of vortex polarization in greater detail.

Intuitively, polarized vortex tangle can be viewed as a set of vortex bundles, so that in each bundle the vortex filaments have the same preferential direction. The simplest way to achieve such a polarization is to subject the system to an external rotation or shear. However, as we will see below, even isotropic and homogeneous turbulence can be, and often is, polarized.

Let us formalize this picture by giving a mathematical definition of the vortex tangle polarization. Consider a circular disk of radius R with randomly selected position of its center and its orientation in the three-dimensional (3D) space. The velocity circulation over the contour of this disk, $\Gamma(R)$, is obviously equal to the quantum circulation κ [see Eq. (5)] multiplied by the difference between the number of vortices crossing the disk in the positive and negative directions with respect to the normal to the disk,

$$\Gamma(R) = \kappa(N_+ - N_-). \quad (1)$$

The totally unpolarized system is represented by a vortex tangle, in which every vortex line consists of a chain of small uncorrelated segments (as in Ref. 19). In this case, the disk crossings would be completely random, and the mean value of Γ^2 would be determined from the central-limit theorem. Namely, if the sign of each crossing is completely random

and statistically independent of all the other crossings, then the total circulation Γ has zero mean and the standard deviation is equal to the standard deviation for the circulation of an individual crossing κ^2 times the total number of terms in the sum (i.e., the number of crossings),

$$\langle \Gamma^2 \rangle = \kappa^2 \langle N_+ + N_- \rangle \sim \kappa^2 (R/\ell)^2, \quad (2a)$$

where ℓ is the mean intervortex distance. We say that this state has zero polarization, $P=0$. Thus, the polarization P can be defined as a degree of deviation from this unpolarized state. For example, in the completely polarized system, all vortex lines would be in a perfectly aligned state, e.g., $N_- = 0$ and $N_+ > 0$, so that

$$\langle \Gamma^2 \rangle = \kappa^2 \langle N_+^2 \rangle \sim \kappa^2 (R/\ell)^4. \quad (2b)$$

We say that in this state $P=1$. Let us now define polarization P by interpolating between these two limits. Namely, we will assume that the system is in a scaling state such that

$$\langle \Gamma^2 \rangle = \kappa^2 \langle N_+^2 \rangle \sim \kappa^2 (R/\ell)^\sigma, \quad (3a)$$

with some constant index σ . Then, for this state, the polarization is defined as

$$P = \sigma/2 - 1. \quad (3b)$$

Note that, in principle, one can have a vortex system in which $P < 0$, e.g., an ordered grid structure composed of alternating positive and negative vortices. However, the alternating periodic structures are unstable and would quickly break up due to reconnections.

Polarization of turbulent states with power-law spectra is considered in Appendix B, describing three different cases. For very steep spectra, $P=1$; for very shallow spectra (including the thermodynamic state), $P=0$; and for intermediate spectra (including K41), P depends on the spectral slope and, therefore, contains a nontrivial information about the turbulent scalings. For K41 turbulence, we have

$$\langle \Gamma^2 \rangle_{K41} \sim \varepsilon^{2/3} R^{8/3}. \quad (4)$$

In this case, $\langle \Gamma^2 \rangle$ can also be obtained from the dimensional analysis. Thus, for K41 turbulence, we have $\sigma=8/3$ and polarization $P=1/3$.

Therefore, the vortex tangle associated with the K41 cascade state is polarized. Note that in the presence of bottleneck (described below) there will also be a contribution of the thermalized part of the spectrum. However, this part is much less than that of the K41 contribution for large R/ℓ . On the other hand, at scale $R \sim \ell$ (and obviously for $R < \ell$), the notion of polarization becomes vague and useless, so one should not attempt to find P for these scales.

Significant polarization associated with K41 cascade at large scales leads to grouping of the adjacent vortex lines into bundles with predominantly parallel orientation, which obviously inhibits reconnections and which selects Kelvin waves to be the dominant carrier of the downscale energy cascade. This picture is self-consistent because, as we will see later, only weak Kelvin waves are needed to carry the energy cascade of the same strength as in the large-scale K41 part. Associated with such weak waves, small bending angles will not allow the adjacent (collinear) vortex lines to ap-

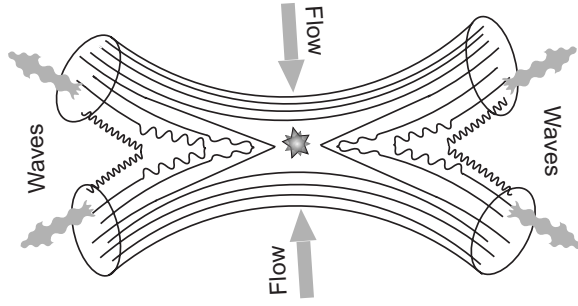


FIG. 2. A sketch of typical reconnection of vortex lines in polarized vortex tangles. A clash of two vortex bundles results in a localized reconnection region. Kelvin waves generated by the reconnections propagate away from the localized reconnection region and spread in space along the vortex lines.

proach each other and reconnect. On the other hand, it should be emphasized that the dominance of Kelvin waves over the vortex reconnections still remains a hypothesis, even though a very plausible one. In this picture, the regions of reconnections are intermittent and limited to locations where two vortex bundles clash, see Fig. 2. Kelvin waves generated by such localized reconnections will spread in space along the vortex lines into the vortex bundles. Therefore the resulting wave distributions will be much less localized in space than the reconnections. Note also that the reconnections in this picture do not lead to a creation of vortex loops of size ℓ or less and, therefore, cannot trigger a cascade of further fragmentation of such loops, as would be the case in unpolarized tangles in counterflow experiments.¹⁹ Assuming that the large-scale dynamics of strongly polarized systems is similar to the classical flows described by Euler equations, one could imagine a classical prototype process in which reconnections will intermittently occur in locations of (yet to be proven to exist) singularities of the Euler equations. One can also see a clear analogy with reconnections of magnetic field lines in magnetohydrodynamics with Alfvén or whistler waves being similar to Kelvin waves.

II. KINETICS OF INTERACTING KELVIN WAVES

Let us describe the statistics of Kelvin waves on thin vortex filaments and their role as a carrier of the energy cascade at scales less than the interline separation ℓ . Here, we briefly give an overview of the results of Kozik and Svistunov on this problem¹² (hereafter referred to as KS-04) with modifications and clarifications, particularly keeping an explicit account of the logarithmic factors which will be important for the effects found in our work. The motion of the tangle of quantized vortex lines can be described by the Biot-Savart equation^{1,2} (BSE) for the time evolving radius vector of the vortex line element $s(\xi, t)$, depending on the arc lengths ξ and time t . When the typical interline spacing ℓ is large in the sense $\Lambda = \ln(\ell/a_0) \gg 1$ (a_0 is the vortex core radius), this equation can be simplified by the so-called local induction approximation (LIA).²⁰ Both BSE and its LIA can be written in the Hamiltonian form.¹⁶

$$i\kappa\dot{w} = \delta H\{w, w^*\}/\delta w^*,$$

where $w(z, t) = x(z, t) + iy(z, t)$, with x and y being small distortions of the almost straight vortex line along the Cartesian z axis. The BSE and LIA Hamiltonians are

$$H^{\text{BSE}} = \frac{\kappa^2}{4\pi} \int \frac{\{1 + \text{Re}[w'^*(z_1)w'(z_2)]\} dz_1 dz_2}{\sqrt{(z_1 - z_2)^2 + |w(z_1) - w(z_2)|^2}}, \quad (5a)$$

$$H^{\text{LIA}} = \frac{\kappa^2 \Lambda}{2\pi} \int \sqrt{1 + |w'(z)|^2} dz,$$

$$\kappa = 2\pi\hbar/m, \quad (5b)$$

where primes denote the z derivatives, κ is the quantum of velocity circulation, and m is the particle mass. Without the cutoff, the integral in H^{BSE} [Eq. (5a)] would be logarithmically divergent, with the dominant contribution given by the leading order expansion of the integrand in small $z_1 - z_2$, which corresponds to H^{LIA} [Eq. (5b)].

It is well known that LIA represents a completely integrable system and it can be reduced to one-dimensional nonlinear Schrödinger equation by Hasimoto transformation.²¹ However, it is the complete integrability of LIA that makes it insufficient for describing the energy cascade and which makes it necessary to consider the next order corrections within the BSE model.

Assuming that the Kelvin wave amplitudes are small with respect to their wavelengths, i.e., $w' \ll 1$ [the self-consistency of this assumption is checked by an estimate of the nonlinearity parameter, see Eq. (16)], we can expand the Hamiltonians (5) in powers of w'^2 : $H = H_0 + H_2 + H_4 + H_6 + \dots$. Next step is to consider a periodic system with the period length \mathcal{L} ($\mathcal{L} \rightarrow \infty$ to be taken later) and to use the Fourier representation $w(z, t) = \kappa^{-1/2} \sum_k a(k, t) \exp(ikz)$, in terms of which the Hamiltonian equation takes the canonical form

$$i\partial a(k, t)/\partial t = \delta \mathcal{H}\{a, a^*\}/\delta a(k, t)^*$$

with a new Hamiltonian $\mathcal{H}\{a, a^*\} = H\{w, w^*\}/\mathcal{L} = \mathcal{H}_2 + \mathcal{H}_4 + \mathcal{H}_6 + \dots$. With $a_j = a(k_j, t)$:

$$\begin{aligned} \mathcal{H}_2 &= \sum_k \omega_k a(k) a^*(k), & \mathcal{H}_4 &= \frac{1}{4} \sum_{12,34} T_{12,34} a_1 a_2 a_3^* a_4^*, \\ \mathcal{H}_6 &= \frac{1}{36} \sum_{123,456} W_{123,456} a_1 a_2 a_3 a_4^* a_5^* a_6^*. \end{aligned} \quad (6)$$

Here, ω_k is the Kelvin wave frequency, and interaction amplitudes $T_{12,34}$ and $W_{123,456}$ are functions of $k_1 \dots k_4$ and $k_1 \dots k_6$, correspondingly. Summations over $k_1 \dots k_4$ in \mathcal{H}_4 and over $k_1 \dots k_6$ in \mathcal{H}_6 are constrained by $k_1 + k_2 = k_3 + k_4$ and $k_1 + k_2 + k_3 = k_4 + k_5 + k_6$, correspondingly. One gets for functions in the Hamiltonians:

$$\omega_k^{\text{BSE}} = \kappa \Lambda(k) k^2 / 4\pi, \quad \Lambda(k) = \ln(1/ka_0),$$

$$T_{1,2,3,4}^{\text{BSE}} = k_1 k_2 k_3 k_4 [\Lambda(k_{\text{cf}}) + F_{1,2,3,4}] / 4\pi,$$

$$W_{1,2,3;4,5,6}^{\text{BSE}} = 9k_1k_2k_3k_4k_5k_6[\Lambda(k_{\text{ef}}) + F_{1,2,3;4,5,6}]/32\pi\kappa, \quad (7a)$$

$$\omega_k^{\text{LIA}} = \kappa\Lambda k^2/4\pi, \quad T_{1,2;3,4}^{\text{LIA}} = \kappa\Lambda k_1k_2k_3k_4/4\pi,$$

$$W_{1,2,3;4,5,6}^{\text{LIA}} = 9\Lambda k_1k_2k_3k_4k_5k_6/32\pi\kappa. \quad (7b)$$

Here, k_{ef} is a mean value of wave vectors in the game and all functions F are of the order of unity; they depend of the ratios of involved k_j to k_{ef} .

It is well known that four-wave dynamics in the one-dimensional case with dispersion laws ω_k^{BSE} or ω_k^{LIA} is absent because the conservation laws of energy and momentum allow only trivial processes with $k_1=k_3$, $k_2=k_4$, or $k_1=k_4$, $k_2=k_3$. However, nontrivial six-wave scattering processes of $3 \rightarrow 3$ type are allowed. For weakly interacting waves, this dynamics can be described in terms of correlation functions $\langle |a(k,t)|^2 \rangle = \mathcal{L}^{-1}n(k,t)$, with the help of a classical six-wave kinetic equation,¹² shown below for the continuous limit $\mathcal{L} \rightarrow \infty$ and $n_j = n(k_j, t)$:

$$\begin{aligned} \frac{\partial n_k}{\partial t} = & \frac{\pi}{12} \int |\tilde{W}_{k,1,2;3,4,5}|^2 [\mathcal{N}_{3,4,5;k,1,2} - \mathcal{N}_{k,1,2;3,4,5}] \delta(\omega_k + \omega_1 \\ & + \omega_2 - \omega_3 - \omega_4 - \omega_5) \delta(k + k_1 + k_2 - k_3 - k_4 - k_5) \\ & \times dk_1 dk_2 \cdots dk_5, \end{aligned} \quad (8)$$

$$\mathcal{N}_{1,2,3;4,5,6} = n_1 n_2 n_3 (n_4 n_5 + n_4 n_6 + n_5 n_6).$$

Here, \tilde{W} is the *full* interaction amplitude that includes the bare six-wave amplitude W and 72 contributions of the second order in the four-wave amplitudes of the order of $T_{k,1,2,3}^2/\omega_k$. Notably, LIA has infinitely many integrals of motion due to its complete integrability. These integrals totally preserve the system from dynamical evolution: $\partial n(k,t)/\partial t = 0$ for any $n(k)$ distribution. With six-wave kinetic Eq. (8), this is possible only if $\tilde{W}_{k,1,2;3,4,5}^{\text{LIA}} = 0$ on the resonant manifold $k+k_1+k_2=k_3+k_4+k_5$ and $\omega_k + \omega_1 + \omega_2 = \omega_3 + \omega_4 + \omega_5$. This means that the leading contribution to $\tilde{W}_{k,1,2;3,4,5}^{\text{BSE}}$, proportional to Λ (that coincides with $\tilde{W}_{k,1,2;3,4,5}^{\text{LIA}}$), also vanishes due to cancellations of the leading contribution to $W_{k,1,2;3,4,5}^{\text{BSE}}$ with that originating from the perturbative terms. Remaining terms in $\tilde{W}_{k,1,2;3,4,5}^{\text{BSE}}$ can be presented as follows

$$\tilde{W}_{k,1,2;3,4,5}^{\text{BSE}} = k_1 k_2 k_3 k_4 k_5 k_6 \Phi_{1,2,3;4,5,6}/4\pi\kappa, \quad (9)$$

where some dimensionless function $\Phi_{1,2,3;4,5,6}$ is of the order of unity and depends only on mutual ratios of k vectors $k_1 \cdots k_6$. This estimate differs from Eq. (7a) for $W_{k,1,2;3,4,5}^{\text{BSE}}$ by the absence of the large factor Λ .

The kinetic equation (8) written for a single vortex filament has a stationary solution¹² with a constant energy density (per unit length) flux ϵ . We reformulate this ‘‘KS-04’’ spectrum to the 3D vortex tangle system in terms of the rate of energy density (per unit mass) in the 3D space, $\epsilon = \epsilon/\rho\ell^2$ (ρ is the fluid density):

$$n_k \simeq (\ell^2 \epsilon)^{1/5} \kappa^{2/5} |k|^{-17/5} \quad \text{KS-04 spectrum.} \quad (10)$$

It should be mentioned, though, that the theory of the cascade energy spectrum (KS-04) was derived with an assumption that vortex lines in the tangle are not rectilinear and noninteracting. In the present work, having in mind that reconnections are dominated by the mean intervortex distance, we silently assumed that the interactions and nonrectilinearity of vortex lines become unimportant at small scales.

III. WARM CASCADES IN HYDRODYNAMIC TURBULENCE

The energy density per unit mass for Kelvin waves of small amplitude is

$$\mathcal{E} = L \int \frac{\omega_k n_k dk}{2\pi} = \int \frac{\mathcal{E}_k dk}{2\pi},$$

where $L \simeq \ell^{-2}$ is the vortex line density per unit volume and \mathcal{E}_k is the one-dimensional energy density in k space. Together with Eq. (10), this gives

$$\mathcal{E}_k \simeq \Lambda (\kappa^7 \epsilon / \ell^8)^{1/5} |k|^{-7/5}. \quad (11)$$

Note that the parameters ϵ and ℓ in Eq. (11) are mutually dependent. Their relation follows from the expression for the mean vorticity in the system of quantum filaments, $\langle |\omega| \rangle \simeq \kappa L \simeq \kappa \ell^{-2}$, where $\langle |\omega| \rangle$ is dominated by the classical-quantum crossover scale and its estimate is usually based on the K41 spectrum,

$$\mathcal{E}_k^{\text{K41}} \simeq \epsilon^{2/3} |k|^{-5/3}, \quad (12)$$

which gives

$$\langle |\omega| \rangle^2 \sim \int^{1/\ell} k^2 \mathcal{E}_k^{\text{K41}} dk \sim \epsilon^{2/3} \ell^{-4/3} \quad \text{or} \quad \epsilon \sim \kappa^3 / \ell^4.$$

However, this estimate is rather unprecise because the K41 spectrum cannot be matched to the Kelvin wave spectrum [Eq. (11)] at the crossover scale and, as is explained below, there exists a bottleneck. However, since the bottleneck is on the classical side of the spectral range, and the mean vorticity is still dominated by the crossover scale, one can find the correct relation between ϵ and ℓ based on Eq. (11) instead of K41. This gives

$$\langle |\omega| \rangle^2 \sim 1/\ell^3 \mathcal{E}_k|_{k=1/\ell} \sim \Lambda (\kappa^7 \epsilon / \ell^{16})^{1/5} \quad \text{or} \quad \epsilon \sim \kappa^3 / \Lambda^5 \ell^4.$$

This estimate is different from the standard one based on K41 by a large factor of Λ^5 .

Now, from Eqs. (11) and (12), one can find the ratio of quantum and classical (K41) spectra of turbulence at the crossover scale $k \simeq 1/\ell$:

$$\mathcal{E}_{1/\ell} / \mathcal{E}_{1/\ell}^{\text{K41}} \simeq \Lambda^{10/3} \gg 1. \quad (13)$$

This ratio shows that quantum turbulence of Kelvin waves requires much higher level of energy (by factor $\Lambda^{10/3}$), in order to provide the same rate of the energy flux (and the same rate of the energy dissipation), than in the hydrodynamic turbulence of classical fluid. The main reason for that is the ‘‘rigidity’’ of the vortex filaments, which is reflected by

factor Λ_k in Eq. (7a) in the Kelvin wave frequency. This contributes a factor of $\Lambda^{8/3}$ into the ratio (13). The remaining factor of $\Lambda^{2/3}$ originates from the fact that any one-dimensional system of interacting Kelvin waves described by the Bio-Savart equation is close to the fully integrable LIA system, in which the dynamics of wave amplitudes is absent. Thus, in order to have the same value of the energy flux and continuity of the spectrum at the crossover scale, there must be a bottleneck pileup of the classical spectrum near this scale by a factor of $\Lambda^{10/3}$, and this will be described by a “warm cascade” solution in what follows.

As we explained, the energy flux carried by classical hydrodynamic turbulence with K41 spectrum (12) cannot fully propagate through the crossover region. Therefore, hydrodynamic motions with larger scales (smaller wave-vectors) will increase their energy up to the level $\mathcal{E}_{1/\ell}$, required for Kelvin waves to maintain the same energy flux. As a result, for $k \leq 1/\ell$, the spectrum of hydrodynamic turbulence, $\mathcal{E}_k^{\text{HD}}$, will not have the K41 scale-invariant form $\mathcal{E}_k^{\text{K41}}$ given by Eq. (12). To get a qualitative understanding of the resulting bottleneck, we will use the so-called warm cascade solutions found in Ref. 14. These solutions follow from the Leith-67 differential model for the energy flux of hydrodynamical turbulence,

$$\varepsilon_k = -\frac{1}{8} \sqrt{|k|^{13} F_k} \frac{dF_k}{dk}, \quad F_k = \frac{\mathcal{E}_k^{\text{HD}}}{k^2}, \quad (14)$$

where F_k is the three-dimensional spectrum of turbulence. Generic spectrum with a constant energy flux is found as the solution to the equation $\varepsilon_k = \varepsilon$:

$$F_k = \left[\frac{24\varepsilon}{11|k|^{11/2}} + \left(\frac{T}{\pi\rho} \right)^{3/2} \right]^{2/3}. \quad (15)$$

The large k range describes a thermalized part of the spectrum with equipartition of energy characterized by an effective temperature T , namely, $T/2$ of energy per degree of freedom; thus, $F_k = T/\pi\rho$ and $\mathcal{E}_k = Tk^2/\pi\rho$. At low k , Eq. (15) coincides with K41 spectrum [Eq. (12)].

This warm cascade solution describes the reflection of K41 cascade and the stagnation of the spectrum near the bottleneck scale, which, in our case, corresponds to the classical-quantum crossover scale. To obtain the spectrum in the classical range of scales, it remains now to find T by matching Eq. (15) with the value of the Kelvin wave spectrum at the crossover scale $\mathcal{E}_k \sim \kappa^2/\ell$. This gives $T/\rho \sim \kappa^2 \ell \sim (\kappa^{11}/\Lambda^5 \varepsilon)^{1/4}$.

Obviously, the transition between the classical and quantum regimes is not sharp and, in reality, we should expect a gradual increase of the role of the self-induced wavelike motions of individual vortex lines with respect to the collective classical-eddy type of motions of the vortex bundles. Thus, the high-wave-number part of the thermalized range is likely to be wave rather than eddy dominated. However, the energy spectrum for this part would still be of the same k^2 form corresponding to the thermal energy equipartition. This picture relies on the assumption (justified below) that the self-induced wave motions have small amplitudes and, therefore, do not lead to reconnections.

The resulting spectrum including both the classical, the quantum, and the crossover parts is shown in Fig. 1 as a log-log plot. It is important to note that at $k > 1/\ell$, in addition to the cascading energy associated with Kelvin waves, there is also an energy associated with the tangle of vortex filaments (shown in Fig. 1 by a green dash-dotted line). The energy spectrum of this part, $\sim |k|^{-1}$, is simply a spectrum associated with a singular distribution of vorticity along one-dimensional curves in the 3D space¹⁰ and does not support a downscale cascade of energy. The cascading and noncascading parts have similar energies at the crossover scale; that is, the wave period and the amplitude are of the order of the characteristic time and size of evolving background filaments. In other words, the scales of the waves and of the vortex “carcass” are not separated enough to treat them as independent components. This justifies the matching of the classical spectrum at the crossover scale with the Kelvin wave part alone ignoring the “carcass,” which is valid up to an order-one factor. This also justifies the way of connecting the carcass spacing ℓ to the cascade rate ε .

IV. WEAKNESS OF TURBULENCE AT AND BELOW SCALE ℓ

In principle, turbulent fragmentation cascade into decreasingly small vortex loops can be an alternative to Kelvin waves as a mechanism of the energy transfer below scale ℓ . Dimensionally, one can obtain spectrum $\propto |k|^{-1}$, which corresponds to such a cascade^{16,22} (and which accidentally coincides with the noncascading carcass spectrum discussed above). The probability of such small-scale reconnections depends on statistics of vortex orientations and can be estimated only in the simplest case of totally unpolarized vortex tangle by adopting a model in which every vortex line consists of short correlated pieces, see, e.g., Ref. 19. This model is relevant for turbulence produced by a thermal counterflow, but not to the case of polarized turbulence produced by classical means. Definitely, in the case when, at the microscopic level, the vortex lines are preferably parallel (presumably this is the case for superfluid turbulence in the rotating tank⁵⁻⁷), the reconnection scenario^{16,22} is irrelevant, as we assumed in our approach.

This picture is supported by an estimation of the nonlinearity parameter ξ_k through comparison of the nonlinear frequency shift $\Delta\omega_k$ with the frequency itself:

$$\xi_k = \frac{\Delta\omega_k}{\omega_k} \simeq \frac{T_{k,k;k}^{\text{BSE}} n_k k}{\omega_k^{\text{BSE}}} \simeq \frac{1}{\Lambda(k\ell)^{2/5}}, \quad (16)$$

which is obtained using Eqs. (7a) and (10) and our estimate $\varepsilon \sim \kappa^3/\Lambda^5 \ell^4$. Now we see that at the crossover scale the nonlinearity is small:

$$\xi_{1/\ell} \simeq 1/\Lambda \simeq 1/\ln(\ell/a_0) \ll 1.$$

Correspondingly, characteristic values of the bending angle α associated with Kelvin waves are also small,

$$\alpha \sim \sqrt{\xi} \sim 1/\sqrt{\Lambda} \ll 1. \quad (17)$$

Hence, the KS-04 weakly nonlinear spectrum should dominate the Svistunov-95 reconnection spectrum.¹⁶ Indeed, the

mean wave amplitude at scale ℓ is $\sim \alpha \ell$, i.e., too small for the adjacent vortex lines to “touch” and reconnect. This proves the self-consistency of the picture of the cascade carried out by interacting Kelvin waves without reconnections, but we emphasize that this picture assumes polarization of the vortex system on which Kelvin waves propagate.

Similarly, in the thermalized region of scales, the mean bending angle can be estimated as $\alpha \sim \sqrt{\xi} \sim (k\ell)^3 / \sqrt{\Lambda} \ll 1$. Thus, the self-induced vortex line motions gradually arising from the eddylike collective motions in the thermalized part take the form of weakly nonlinear Kelvin waves. The nonlinearity of Kelvin waves grows with k in the thermalized part, reaching its peak at the crossover scale and decreasing in the Kelvin cascade range.

V. SUMMARY AND DISCUSSION

In this paper, we suggested the following route for the development of the energy cascade: K41 \rightarrow “warm up” \rightarrow KS-04 spectrum with a very pronounced bottleneck effect. This scenario is relevant for *polarized* vortex systems resulting from forcings of a classical type, e.g., a towed grid or rotation, but not relevant to unpolarized vortex tangles produced by thermal counterflows. In our arguments, we relied on the fact that polarization suppressed the reconnection-fragmentation cascade. Classically produced K41 turbulence is indeed polarized. However, its polarization is not perfect and, at this time, we cannot exclude that in some specific cases the reconnection dynamics can suppress the bottleneck accumulation of energy.

In this paper, we predicted that the bottleneck at the classical-quantum crossover scale amplifies the spectrum at this scale by a large factor of $\Lambda^{10/3}$ with respect to K41. Correspondingly, the corrected estimate for the crossover scale which takes this bottleneck into account is $\ell \sim (\kappa^3 / \Lambda^5 \epsilon)^{1/4}$, which is $\Lambda^{5/4}$ times smaller than the standard estimate based on K41. Yet another way to reformulate the same thing would be to say that the effective viscosity ν' is reduced by a large factor of Λ^5 , i.e.,

$$\nu' \approx \kappa / \Lambda^5 \quad (18)$$

(see, e.g., Ref. 3 for definition of ν' and explanation of its meaning).

A comment is due about the locality of the transition between the classical turbulence and the Kelvin wave cascade. Due to a sharp kinklike nature of the vortex reconnections generating Kelvin waves (see Fig. 2), one might think that the energy is injected into the Kelvin wave cascade over a wide range of wave numbers (associated with a Fourier analysis of the kink) and conclude that the energy spectrum in the quantum region should differ from $k^{-7/5}$. However, as was shown in Ref. 15, the Fourier transform of the kink decays with k fast enough for the direct cascade scaling to dominate. In other words, the reconnection forcing appears to be more or less equivalent to a low-frequency forcing at the intervortex scale ℓ .

To describe the shape of the bottleneck spectrum, we used the warm cascade solution previously obtained in Ref. 14 based on the Leith-67 differential model Eq. (14), as it is the

simplest model which can provide a clear qualitative understanding of the bottleneck phenomenon. Clearly, the differential model Eq. (14) exaggerates the locality of the interactions of scales in real Navier-Stokes turbulence, where the main contribution to evolution of $\mathcal{E}_k^{\text{HD}}$ originates from a wider range of comparable scales $q \sim k$. Some authors claim that extended interaction triads with q between k/A and Ak (with $A \sim 10$) are most important.²³ If so, the transient region between K41 and the spectra in thermodynamic equilibrium can be wider than the one predicted by the differential approximation Eq. (14). To account for this effect, one can use a more sophisticated turbulence closure based on an integral rather than a differential equation, e.g., one of the traditional closures such as the direct interaction approximation or eddy-damped quasinormal Markovian (EDQNM), as was done in Ref. 24, or even simpler closure, suggested in Appendix A.

In this paper, we did not consider the effects of the mutual friction between the normal and superfluid components, thereby restricting our consideration to low temperatures (e.g., below 1 K for ^4He). At higher temperatures, the dissipation of energy by the mutual friction can exceed the energy transfer to Kelvin waves, which would make our analysis and conclusions inapplicable. This seems to be the case, for example, in experiments described in Ref. 11.

At lower temperatures, there is a clear lack of experiments on turbulence generated by classical means. In this respect, one could mention the ^3He experiment on turbulence generated by a vibrating wire at Lancaster,⁴ the authors of which found the value of the effective viscosity $\nu' = 0.2\kappa$, which appears to be much greater than our prediction (18). On the other hand, to obtain this value, the authors used an estimate for the integral (energy containing) scale to be equal to the thickness of the turbulent region, $d = 1.5$ mm, which in our opinion may not be the case for the oscillating grid setup. Lacking direct measurements of d , we could get guidance from the oscillating grid experiments in classical fluids, see, e.g., Ref. 27, where the following estimate for the integral scale is given:

$$d = 0.25(S/M)^{1/2} z,$$

where M is the mesh size, S is the amplitude of oscillations, and z is the distance from the grid. Taking the Lancaster parameters, $M = 50 \mu\text{m}$, $S = 1 \mu\text{m}$, and $z = 1.5$ mm, we get $d = 50 \mu\text{m}$. Estimating ν' with this value of the integral scale would give $\nu' \sim 2 \times 10^{-4} \kappa$, which would be consistent with the small Λ^{-5} coefficient in Eq. (18). However, it is not possible to be more conclusive, one way or another, without more direct measurements of the turbulent parameters in this case.

A lucky exception appears to be a different ^3He experiment on rotation generated turbulence, in which the bottleneck phenomenon appears to be important in understanding the observed propagation speed of the turbulent-laminar interface, see Ref. 25 for detailed explanations.

In the final stages of modifying our paper, our attention was drawn to a different preprint²⁸ where an alternative picture of the crossover turbulence was presented with bottleneck being prevented by reconnections. The authors argued

that the self-induced part of the vortex line velocity becomes larger than the classical collectively produced velocity in the vortex bundle already at the scale $r_0 \sim \Lambda^{1/2} l_0 \gg l_0$. From this, they concluded that the polarized vortex bundles move randomly with respect to each other, which leads to their random reconnections. In this respect, we would like to reemphasize our view that the fast self-induced motions take the form of rapidly oscillating Kelvin waves rather than of a chaotic motion of vortex bundles. Moreover, as expressed in our estimate (17), these Kelvin waves must have very small bending angles ($1/\Lambda^{1/2}$ or less) in order for the six-wave Kelvin cascade to carry the same flux as in the K41 (large-scale) part of the spectrum. Such small bending angles are insufficient for the neighboring lines within a particular bundle to approach each other and to reconnect neither in the thermalized nor in the cascade range of scales. Thus, reconnections are limited to rather small volumes in between colliding large-scale bundles.

On the other hand, as we have already said in this paper, polarization of K41 turbulence is not perfect and we may expect reconnections to play some role which would lead to certain modifications of the bottleneck phenomenon described in this paper. Relative role of the reconnections versus the Kelvin wave cascades is also likely to depend on the particular way of exciting turbulence. In particular, we may expect further reinforcement of the polarization, and therefore, stronger suppression of reconnections, in rotating systems and in systems with a strongly sheared mean flow.

ACKNOWLEDGMENTS

The authors are thankful to S. Nemirovskii, B. Svistunov, and W. F. Vinen for fruitful discussions. V.L. is grateful to G. Volovik, M. Krusius, and V. Eltsov for involving him into a discussion of ongoing experiment (Ref. 25) on turbulence in superfluid ^3He , which shed light on the bottleneck problem. The work is partially supported by the US-Israel Binational Science Foundation and by Finberg Foundation for O.R. In part, this work was done during the EPSRC sponsored Warwick Turbulence Symposium 2005-2006, which comprised a series of workshops on different aspects of turbulence and a year-long visitor program.

APPENDIX A: SIMPLE TURBULENT CLOSURE

Here, we propose a different model which could be viewed as the simplest (minimal) integral closure to be used in the future for an improved description of the transitional bottleneck region. The model comprises in writing the collision term $\text{St}\{F_k\}$ in energy spectrum balance $F_k/t = \text{St}\{F_k\}$ as follows:

$$\begin{aligned} \text{St}\{F_k\} \simeq & \int_{-\infty}^{\infty} \frac{q^2 dq p^2 dp \delta(k+q+p)}{2\pi k^2 (k^2 + q^2 + p^2)} k [k F_q F_p + q F_k F_p \\ & + p F_q F_k] / (\gamma_k + \gamma_q + \gamma_p), \end{aligned} \quad (\text{A1})$$

where k , q , and p are one-dimensional vectors varying in the interval $(-\infty, +\infty)$, and $\gamma_k = \sqrt{|k|^5 F_k}$ represents eddy-turnover frequency. The model (A1) differs from EDQNM by replace-

ment of $d^3 q d^3 p \delta^3(\mathbf{k} + \mathbf{q} + \mathbf{p})$ with three-dimensional vectors \mathbf{k} , \mathbf{q} , and \mathbf{p} by $q^2 dq p^2 dp \delta(k+q+p)/(k^2 + q^2 + p^2)$ with one-dimensional vectors, by a simpler form of γ_k , and by one-dimensional version of the interaction amplitude ($V_{kqp}^{\alpha\beta\gamma} \Rightarrow k$).

The model (A1) satisfies all general closure requirements: it conserves energy, $\int k^2 \text{St}\{F_k\} dk = 0$ for any F_k , and $\text{St}\{F_k\} = 0$ on the thermodynamic equilibrium spectrum $F_k = \text{const}$ and on the cascade spectrum $F_k \propto |k|^{-11/3}$. Importantly, the integrand in Eq. (A1) has the correct asymptotical behavior at the limits of small and large q/k as in the sweeping-free Belinicher-L'vov representation, see Ref. 26. This means that our model adequately reflects contributions of the extended interaction triads and thus should be useful in the future for a quantitative description of the transient region between turbulent spectra with thermodynamic and energy-flux equilibria.

APPENDIX B: VELOCITY CIRCULATION AND POLARIZATION IN TURBULENCE

In this appendix, we will calculate the velocity circulation Γ over a circular contour of radius R in classical turbulence with a power-law spectrum. Let the second order velocity correlation function (3D spectrum) in the k space for isotropic homogeneous turbulence be

$$F_k = C_F \frac{v_T^2 k_*^{x-3}}{k^x}, \quad (\text{B1})$$

where $C_F = 2\pi^2 |x-3|$, v_T is the rms velocity in turbulence, and k_* is a wave number of truncation from above for $x < 3$ (e.g., for the thermodynamic equilibrium with $x=0$) and from below for $x > 3$ (e.g., for K41 turbulence with $x=11/3$). Such a truncation is necessary for v_T to be finite, and we will see below that the $x=3$ boundary also separates different types of the scaling behavior of the velocity circulation.

Consider the circulation

$$\Gamma = \int_R \omega_n d^2 r, \quad (\text{B2})$$

where $\omega = \nabla \times \mathbf{v}$ is vorticity, and the integral is taken around an arbitrary circle of radius R . Then

$$\langle \Gamma^2 \rangle = \int_R \int \langle \omega_{1,n} \omega_{2,n} \rangle d^2 r_1 d^2 r_2. \quad (\text{B3})$$

Due to isotropy of the turbulence, we may approximate $\langle \omega_{1,n} \omega_{2,n} \rangle = \frac{1}{3} \langle \boldsymbol{\omega}_1 \cdot \boldsymbol{\omega}_2 \rangle$. With $\mathbf{r}_{12} = \mathbf{r}_1 - \mathbf{r}_2$ and $\langle \boldsymbol{\omega}_{k_1} \cdot \boldsymbol{\omega}_{k_2} \rangle = 2k_1^2 (2\pi)^3 \delta(\mathbf{k}_1 + \mathbf{k}_2) F_{k_1}$, we have

$$\begin{aligned} \langle \boldsymbol{\omega}_1 \cdot \boldsymbol{\omega}_2 \rangle &= \int \int \frac{d^3 k_1 d^3 k_2}{(2\pi)^6} e^{i(\mathbf{k}_1 \cdot \mathbf{r}_1 + \mathbf{k}_2 \cdot \mathbf{r}_2)} \langle \boldsymbol{\omega}_{k_1} \cdot \boldsymbol{\omega}_{k_2} \rangle \\ &= 2 \int k^2 F_k e^{i\mathbf{k} \cdot \mathbf{r}_{12}} \frac{d^3 k}{(2\pi)^3} = \frac{C_F v_T^2 k_*^{x-3}}{\pi^2 r_{12}} \int_0^\infty \frac{\sin(kr_{12})}{k^{x-3}} dk. \end{aligned} \quad (\text{B4})$$

When $3 < x < 5$, this integral converges and we have

$$\langle \boldsymbol{\omega}_1 \cdot \boldsymbol{\omega}_2 \rangle = 2|x-3| \frac{v_T^2}{r_{12}^2} (k_* r_{12})^{x-3} \left\{ -\mathcal{G}(4-x) \sin \frac{\pi x}{2} \right\}, \quad (\text{B5})$$

where $\mathcal{G}(x)$ is the gamma function. Substituting this expression into Eq. (B3) and integrating, we have

$$\langle \Gamma^2 \rangle = C_x \frac{v_T^2}{k_*^2} (k_* R)^{x-1}, \quad (\text{B6})$$

where C_x is an order-one constant (whose analytical dependence on index x is very complicated).

For $x < 3$, the integral in Eq. (B4) diverges at the upper limit and, therefore, has to be truncated at the maximum wave number, which, in this case, is k_* . We have

$$\langle \boldsymbol{\omega}_1 \cdot \boldsymbol{\omega}_2 \rangle = \frac{C_F v_T^2 (k_* r_{12})^{x-3}}{\pi^2 r_{12}^2} \int_0^{k_* r_{12}} \frac{\sin y}{y^{x-3}} dy. \quad (\text{B7})$$

The integral in this expression can be found in terms of the special functions whose asymptotical behavior can be readily obtained. This way, one can show that the correlator $\langle \boldsymbol{\omega}_1 \cdot \boldsymbol{\omega}_2 \rangle$ decays in r_{12} sufficiently fast, so that for $k_* R \gg 1$, one can pass in the integral (B3) to the symmetric variables $\mathbf{r}_+ = \frac{1}{2}(\mathbf{r}_1 + \mathbf{r}_2)$ and $\mathbf{r}_{12} = \mathbf{r}_1 - \mathbf{r}_2$, use the polar coordinates, and replace the upper integration limit for r_{12} with infinity,

$$\langle \Gamma^2 \rangle = \frac{2\pi^2 R^2}{3} \int_0^\infty \langle \boldsymbol{\omega}_1 \cdot \boldsymbol{\omega}_2 \rangle r_{12} dr_{12}.$$

Substituting $\langle \boldsymbol{\omega}_1 \cdot \boldsymbol{\omega}_2 \rangle$ from Eq. (B7) and integrating, we have

$$\langle \Gamma^2 \rangle = \frac{4\pi^4}{3} v_T^2 R^2. \quad (\text{B8})$$

Interestingly, this expression is independent of both the spectrum exponent x and of the cutoff k_* . This fact has a simple physical interpretation. Suppose that the correlation length of vorticity field in turbulence ℓ_ω is short so that $\ell_\omega \ll R$. Then the circle of radius R embraces $N = R^2/\ell_\omega^2$ random and effectively independent vortex tubes, each having radius $\sim \ell_\omega$ and circulation $\gamma_l \sim v_T \ell_\omega$. Because of the statistical independence of these tubes, $\langle \Gamma^2 \rangle$ can be found using the central limit theorem, similar to the way we did in the main text for the set of random quantized vortex lines. We have

$$\langle \Gamma^2 \rangle \sim \gamma_l^2 N = v_T^2 R^2,$$

which coincides, up to an order-one numerical factor, with expression (B8). Note that dependence on ℓ_ω has dropped out, which corresponds to independence of expression (B8) of x and k_* .

For $x > 5$, the integral in (B4) diverges at the lower limit and, therefore, has to be truncated at the minimum wave number, which, in this case, is again k_* . We have

$$\langle \boldsymbol{\omega}_1 \cdot \boldsymbol{\omega}_2 \rangle = \frac{C_F v_T^2 k_*^2}{\pi^2 (x-5)}. \quad (\text{B9})$$

As we see, this correlator is independent of the distance r_{12} , which simply means that the correlation length in this case is of the order of the maximal length scale $1/k_*$. The integration in Eq. (B3) in this case reduces to the multiplication by the square of the circle area, i.e.,

$$\langle \Gamma^2 \rangle = \frac{1}{3} \frac{C_F v_T^2 k_*^2}{\pi^2 (x-5)} (\pi R^2)^2 = \frac{2\pi^2 (x-3)}{3(x-5)} v_T^2 k_*^2 R^4. \quad (\text{B10})$$

The R^4 scaling here coincides with the one obtained in the main text for a bundle of perfectly aligned (polarized) vortex lines. This is not surprising since the vorticity correlation length in this case $\sim 1/k_*$, which is much greater than the contour size R . Another interesting effect to note is that $\langle \Gamma^2 \rangle$ diverges for $x \rightarrow 5$.

Let us now summarize all the cases. We have

$$x < 3 \text{ (e.g., thermodynamic): } \langle \Gamma^2 \rangle = \frac{4\pi^4}{3} v_T^2 R^2,$$

$$3 < x < 5 \text{ (e.g., K41): } \langle \Gamma^2 \rangle = C_x \frac{v_T^2}{k_*^2} (k_* R)^{x-1},$$

$$x > 5 \text{ (e.g., smooth field): } \langle \Gamma^2 \rangle = \frac{2\pi^2 (x-3)}{3(x-5)} v_T^2 k_*^2 R^4.$$

For polarization P (see definition in the main text), we have respectively

$$P = \begin{cases} 0, & x < 3 \\ (x-3)/2, & x \in (3, 5) \\ 1, & x > 5. \end{cases} \quad (\text{B11})$$

So, the thermal equilibrium state ($x=0$) is not polarized at all, $P=0$, while Kolmogorov turbulence ($x=11/3$) is partially polarized, $P=1/3$.

¹R. J. Donnelly, *Quantized Vortices in He II* (Cambridge University Press, Cambridge, 1991).

²*Quantized Vortex Dynamics and Superfluid Turbulence*, edited by C. F. Barenghi *et al.*, Lecture Notes in Physics Vol. 571 (Springer-Verlag, Berlin, 2001).

³W. F. Vinen and J. J. Niemela, *J. Low Temp. Phys.* **128**, 167 (2002).

⁴S. N. Fisher, A. J. Hale, A. M. Guénault, and G. R. Pickett, *Phys. Rev. Lett.* **86**, 244 (2001).

⁵R. Hänninen, R. Blaauwgeers, V. B. Eltsov, A. P. Finne, M. Krusius, E. V. Thuneberg, and G. E. Volovik, *Phys. Rev. Lett.* **90**, 225301 (2003).

⁶A. P. Finne, T. Araki, R. Blaauwgeers, V. B. Eltsov, N. B. Kopnin, M. Krusius, L. Skrbek, M. Tsubota, and G. E. Volovik, *Nature*

- (London) **424**, 1022 (2003).
- ⁷D. I. Bradley, D. O. Clubb, S. N. Fisher, A. M. Guénault, R. P. Haley, C. J. Matthews, G. R. Pickett, V. Tsepelin, and K. Zaki, *Phys. Rev. Lett.* **95**, 035302 (2005).
- ⁸V. B. Eltsov, A. P. Finne, R. Hänninen, J. Kopu, M. Krusius, M. Tsubota, and E. V. Thuneberg, *Phys. Rev. Lett.* **96**, 215302 (2006).
- ⁹D. I. Bradley, D. O. Clubb, S. N. Fisher, A. M. Guénault, R. P. Haley, C. J. Matthews, G. R. Pickett, V. Tsepelin, and K. Zaki, *Phys. Rev. Lett.* **96**, 035301 (2006).
- ¹⁰T. Araki, M. Tsubota, and S. K. Nemirovskii, *Phys. Rev. Lett.* **89**, 145301 (2002).
- ¹¹S. R. Stalp, J. J. Niemela, W. F. Vinen, and R. J. Donnelly, *Phys. Fluids* **14**, 1377 (2002).
- ¹²E. V. Kozik and B. V. Svistunov, *Phys. Rev. Lett.* **92**, 035301 (2004).
- ¹³W. F. Vinen, M. Tsubota, and A. Mitani, *Phys. Rev. Lett.* **91**, 135301 (2003).
- ¹⁴C. Connaughton and S. Nazarenko, *Phys. Rev. Lett.* **92**, 044501 (2004).
- ¹⁵S. Nazarenko, *JETP Lett.* **84**, 700 (2006).
- ¹⁶B. V. Svistunov, *Phys. Rev. B* **52**, 3647 (1995).
- ¹⁷W. Thomson, *Philos. Mag.* **10**, 155 (1880).
- ¹⁸H. E. Hall, *Proc. R. Soc. London, Ser. A* **245**, 546 (1958).
- ¹⁹S. K. Nemirovskii, *J. Low Temp. Phys.* **142**, 769 (2006).
- ²⁰K. W. Schwarz, *Phys. Rev. B* **31**, 5782 (1985); **38**, 2398 (1988).
- ²¹H. Hasimoto, *J. Fluid Mech.* **51**, 477 (1972).
- ²²W. F. Vinen, *Phys. Rev. B* **61**, 1410 (2000).
- ²³S. A. Orzag, *J. Fluid Mech.* **41**, 363 (1970).
- ²⁴W. J. T. Bos and J.-P. Bertoglio, *Phys. Fluids* **18**, 071701 (2006).
- ²⁵V. B. Eltsov, A. Golov, R. de Graaf, R. Hanninen, M. Krusius, V. L'vov, and R. E. Solntsev, International Workshop on Rotating Superfluid Turbulence, Propagation of Turbulent Front in Rotating Superfluid Turbulence, Jerusalem, April 2007 (unpublished).
- ²⁶V. I. Belinicher and V. S. L'vov, *Zh. Eksp. Teor. Fiz.* **93**, 1269 (1987).
- ²⁷A. Eidelman, T. Elperin, A. Kapusta, N. Kleeorin, A. Krein, and I. Rogachevskii, *Nonlinear Processes Geophys.* **9**, 201 (2002).
- ²⁸E. V. Kozik and B. V. Svistunov, arXiv:cond-mat/0703047v2 (unpublished).